Towards Predicting the Effects of Stent-Grafting on the Motion of the Thoracic Aorta*

Ernst Schwartz[1], Johannes Holfeld[2], Martin Czerny[3], Christian Loewe[4], and Georg Langs[1]

[1] CIR Lab, Department of Radiology, Medical University of Vienna
[2] Department of Cardiac Surgery, Innsbruck Medical University
[3] Department of Cardiovascular Surgery, Bern University Hospital
[4] Department of Radiology, Medical University of Vienna

Abstract. The Thoracic Aorta is a highly dynamic vessel. Changes induced to vessel motion due to procedures such as stent-grafting are hypothesized to play a significant role in the outcome of interventions. A priori knowledge about these effects is difficult to establish due to numerous unknown factors influencing the prognosis. We propose a framework that learns typical changes to vessel wall motion induced by interventions from a set of pre- and post-intervention sequence pairs, and a large set of single sequences. The method uses a combined model of vessel shape, -motion, and stent location to predict post intervention deformation from pre-intervention sequence. Experimental results illustrate the influence of the individual regressors on the prediction accuracy. They indicate that prediction is feasible.

Keywords: Vascular, Aorta, Modeling, Prediction, Treatment planning, Stent-grafting

1 Introduction

The complex topology of the vasculature in the Aortic Arch and its strong movement related to myocardial motion makes the treatment of pathologies in the thoracic aorta a challenging procedure in vascular surgery. Supra-aortic branch transposition [1] followed by stent-grafting has recently been proposed as a promising treatment option. However, the insertion of a stent-graft in this highly dynamic region of the aorta affects the morphological and dynamic properties of the vessel [2]. These changes have been hypothesized to lead to elevated local stress on the vessel wall and in turn to adverse prognosis on the outcome of endovascular interventions [3, 4]. In order to support clinicians in treatment planning, we propose a method to predict movement-related stress in the Thoracic Aorta after the intervention from pre-intervention data. We base our analysis on ECG-gated Computed Tomography Angiography (CTA) sequences as this

* This work was partially funded by the OeNB (13497 AORTAMOTION), EU (257528 KHRESMOI), and Austrian Science Fund FWF (22578-B19 PULMARCH)

modality allows for the extraction of both dynamic and static properties of the aorta.

The remainder of the paper is organized as follows. First, we describe the methods used to extract deformation fields and surface segmentations from the CTA data in Section 2. We use this information in Section 3 to obtain a discriminative description of the global shape of the Thoracic Aorta. Together with pre-intervention shape and motion parameters, these parameters are used to build a regression model of vessel motion after intervention. This is described in Section 4. We present results for a predictive model of stent-grafting procedures in Section 5. Finally, a discussion of open questions and future research directions concludes the paper in Section 6.

2 Preprocessing

The proposed method is based on ECG-gated CTA data [3] whose original voxel size of 0.67 x 0.67 x 0.33 mm is resampled to isotropy of 1mm. We found this resolution to be a reasonable compromise between the level of detail of the analysis and the required processing time. Each acquisition consists of a series $\mathbf{S} = (\mathbf{V}_1, ...\mathbf{V}_T)$ of volumes $\mathbf{V}_t$ representing the thorax of the patients at breath-hold during one cardiac cycle. Registration and segmentation procedures are then applied to the sequence in order to extract dynamic models of the Thoracic Aorta $\mathcal{A}$.

3D+t Registration Group-wise temporal b-spline registration [5] is performed on each CTA sequence to extract myocardial and induced vascular motion. The result of the registration $\mathcal{R}$ is a sequence of vector fields matching each volume $\mathbf{V}_t$ to a hypothetical mean volume. We exploit the fact that the time-point in the cardiac cycle corresponding the first frame in $\mathbf{S}$ is known from the ECG-signal. We resample the displacement fields to yield $\mathcal{R}(\mathbf{S}) = (\mathbf{D}_1, ..., \mathbf{D}_T)$, a smooth sequence of dense vector fields $\mathbf{D}$ each mapping $\mathbf{V}_{t=1...T}$ to $\mathbf{V}_1$. These vector fields can be interpolated at a given position $\mathbf{v}$ and a series of time points t to yield trajectories of this location during the cardiac cycle as $\mathbf{d}(\mathbf{v}, t) = \mathbf{D}_t(\mathbf{v}), \mathbf{v} \in \mathbb{R}^3, t \in [0...T]$.

Segmentation We compute the mean volume $\overline{\mathbf{V}}_{\mathcal{A}} = \frac{1}{T}\sum_{t=1}^{T} \mathbf{V}_t(\mathbf{D}_t^{-1}(x))$ of a sequence which we segment using a tracking-based approach similar to [6]. We represent the resulting segmentation $\mathcal{S}(\overline{\mathbf{V}}_{\mathcal{A}})$ of the aorta as an estimate of the vessel centerline C and the radially sampled surface point parameterization R

$$\begin{aligned} \mathcal{S}(\overline{\mathbf{V}}_{\mathcal{A}}) \ni \mathbf{v}(s,\theta) &= C(s) + R(s,\theta)\boldsymbol{n} \\ s \in [0...1]\ ,\ \theta \in [0...2\pi[\ ,\ \boldsymbol{n} &\cdot dC(s) = 0 \end{aligned} \tag{1}$$

The positioning of surface points in consecutive orthogonal planes of the centerline is optimized to minimize radial drift, resulting in a smooth surface model.

3 Automated Shape-Model Construction

We expect both local and global geometric properties of the vessel to influence the outcome of vascular interventions. In order to encode global properties of the shape of each aorta in the population, we propose to build a low-dimensional representation of the surface models $\mathcal{S}(\mathcal{A}_n), n = 1...N$ using a Statistical Shape Model (SSM) [7].

3.1 Shape Alignment

To align all centerlines C_n in the population, we translate each to the center of its Aortic Arch and assume the closest points $C_n(s = c_n)$ on the centerline to correspond across subjects. The remainders $C_n(s > c_n),\ s \leq 1$ and $C_n(s < c_n),\ s \geq 0$ are resampled to ensure complete overlap. This alignment procedure establishes correspondences among all centerlines $C_n(s)$ of the model population so that $C_i(s) \leftrightarrow C_j(s)\ \ \forall i, j \in [1...N]\ ,\ s \in [0...1]$

3.2 Model construction

We construct the mean centerline $\overline{C} = \frac{1}{N}\sum_{n=1}^{N} C_{\mathcal{A}_n}$ and a linear shape model $C_{\mathcal{A}_n} \approx \overline{C} + \mathbf{\Psi}^{(C)}\boldsymbol{\lambda}_{\mathcal{A}_n}^{(C)}$ for the population of centerlines using PCA, where $\mathbf{\Psi}^{(C)}$ is the eigendecomposition of the covariance matrix of all $C_{\mathcal{A}_n}$ and $\lambda_{\mathcal{A}_n}^{(C)}$ the corresponding modes of variation for a specific aorta $\mathcal{A}_n$.
Because radial correspondences can be assumed as explained in Section 2, we model the radial component R in identical fashion as $R_{\mathcal{A}_n} \approx \overline{R} + \mathbf{\Psi}^{(R)}\boldsymbol{\lambda}_{\mathcal{A}_n}^{(R)}$ where $\overline{R} = \frac{1}{N}\sum_{n=1}^{N} R_{\mathcal{A}_n}$.

In each of the two shape models, we retain the coefficients that explain 95% of the total shape variability in the population. The shape of each aorta $\mathcal{A}_n$ in the population can then be represented as two low-dimensional sets of coefficients $\boldsymbol{\lambda}_{\mathcal{A}_n}^{(C)} \in \mathbb{R}^8$ and $\boldsymbol{\lambda}_{\mathcal{A}_n}^{(R)} \in \mathbb{R}^{26}$ of these shape models.

4 Predicting the Effects of Stent-Grafting

In the previous section, we described how to encode the shape of the aorta in a low-dimensional representation. We will now use these global shape descriptors, as well additional local properties of the aorta before intervention in a regression model to predict its motion after stent-grafting.

4.1 Parameters affecting treatment outcome

We expect three main factors to predict the outcome of endovascular interventions: the shape of the affected vessel, its dynamics before the procedure and the location of the stent-graft. We use the coefficients of the shape model as descriptors of its overall shape, and local features to represent morphological details of each case.

Global shape information The global shape of every $\mathcal{S}(\mathcal{A}_n)$ is encoded using an SSM computed from 54 CTA sequences as described in Sec. 3. The coefficients $\boldsymbol{\lambda}_{\mathcal{A}_n}^{(C)}$ represent the shape of the centerline before the intervention. The coefficients $\boldsymbol{\lambda}_{\mathcal{A}_n}^{(R)}$ encode the mode of radial displacement from the centerline. Concatenating these results in the global shape feature vector $\mathbf{f}_{\text{globalshape}}(\mathcal{A}_n) \in \mathbb{R}^{34}$.

Local shape information For each $\mathbf{v} \in \mathcal{S}(\mathcal{A}_n)$, we compute the surface curvature in terms of its minimum, maximum, mean and gaussian components. Additionally, the distance of each $\mathbf{v}$ to the centerline C and a local estimate of vessel radius are computed. Finally, we compute a shape signature of $\mathcal{S}(\mathcal{A}_n)$ as proposed in [8]. This representation encodes local geometric information at each point in the feature vector $\mathbf{f}_{\text{localshape}}(\mathbf{v}) \in \mathbb{R}^{27}$.

Location relative to stent-graft The location of a stent graft is indicated as a binary variable for each $\mathbf{v}$. In cases where a stent-graft is present, we also compute the distance between every point outside the stent graft and its distal ends which we store as $\mathbf{f}_{\text{stent}}(\mathbf{v}) \in \mathbb{R}^3$.

Motion properties Common methods of describing vascular motions rely on aggregate values for cross-sectional regions of the vessel [9]. However, we expect the changes of vessel movement to be more unevenly distributed. Therefore, we estimate the motion of the aorta on the complete vessel surface represented by $\mathbf{v}$ by interpolating and concatenating the displacement fields $\mathbf{D}_t$. From these raw motion trajectories, we compute information about the Total Distance Travelled (TDT) as $\text{TDT}(\mathbf{v})_{\mathcal{A}} = \int \frac{\partial \mathbf{d}(\mathbf{v},t)}{\partial t} dt$. Furthermore, we compute the maximum distance travelled between two time points and the standard deviation of distances travelled. In order to to include more contextual information about vessel movement in the model, we aggregate information about cross-sections of the vessel. We compute mean and maximum TDT as well as the standard deviation in TDT in each cross-section $C(s)$. In order to reduce the influence of patient condition at the time of acquisition, we normalize each of these values to the interval [0...1]. This results in the local motion features $\mathbf{f}_{\text{motion}}(\mathbf{v}) \in \mathbb{R}^8$.

4.2 Regression Model

Estimating the way in which an intervention affects the motion of the aorta is a highly non-linear and underdetermined problem. We therefore use the recently proposed ensemble-method of Random Forest Regression [10] for model learning. Furthermore, due to limited amount of training data, we aim at predicting TDT instead of the complete vessel movement. We limit the space of training vectors according to a rejection procedure, detailed below.

Random Forests Random Forest Regression is a popular non-linear regression method based on a bootstrapping approach [11]. It uses a series of regression trees that are built from random subsamplings of the training data instances.

The accuracy of each tree is tested based on the remainder of the training set. By computing the average vote of all trees in the forest, regression can be performed on unseen data.

Outlier Removal The effects of stent-grafting in the Aortic Arch are highly non-linear and can vary widely from patient to patient [2]. To reduce the effects of local spurs of aortic motion in single patient we removed all $\mathbf{v}$ from the training set whose TDT was 3 standard deviations larger than the mean in each case. We retained all $\mathbf{v}$ located in the Ascending Aorta, as strong movement in that part of the anatomy is expected.

Prediction model For each surface model point observed before stent-grafting $\mathbf{v} \in \mathcal{S}(\mathcal{A}_{\text{pre}})$ we concatenate the previously described features to form a 75-dimensional feature vector $\mathbf{f}(\mathbf{v})$. Using Random Forests, we learn a regression model $\mathfrak{R}_{\text{RF}}$ between these features and the motion of the Thoracic Aorta $\mathcal{A}_{\text{post}}$ as

$$\text{TDT}(\mathbf{v}') \approx \mathfrak{R}_{\text{RF}}(\mathbf{f}(\mathbf{v}))\ ,\ \mathbf{v} \in \mathcal{S}(\mathcal{A}_{\text{pre}})\ ,\ \mathbf{v}' \in \mathcal{S}(\mathcal{A}_{\text{post}}) \tag{2}$$

5 Results

We applied the proposed model learning method to a set of 4 cases where stent-grafting in the Aortic Arch was performed after supra-aortic rerouting [1]. We perform Leave-One-Out Cross Validation (LOOCV), learn a model from 3 cases and apply it to predict post-intervention motion from pre-intervention feature vectors for the fourth case. We present the results in Figure 3. Subfigure a) shows the TDT of the aorta before the intervention, b) the prediction of TDT using the presented regression model and c) the real measured TDT. As the distribution of values of TDT are skewed due to the strong movement of the AA, we limit the color-coding at +3 standard deviations TDT in each case.

5.1 Importance of model parameters

During regression Random Forests compute the Gini importance score of each parameter in the feature vectors used for training. Figure 2 shows the feature importance in the 4 LOOCV runs we performed. As expected, the most relevant feature for predicting post-intervention TDT changes is the position of the observed sampling point $\mathbf{v}$ on the centerline. The second-most important factor in the 4 observed cases is the distance of the observed point to the stent in the Ascending Aorta, which stems from the strong motion in that part of the vessel. Changes in motion seem further to be strongly influenced by the motion before the intervention, most notably the mean displacement of the corresponding orthogonal plane. According to our experiments, the local shape of the vessel plays a lesser but still significant role in the outcome of the intervention. The information contained in the first 3 components of the spectral signature shows the highest importance of the local shape parameters. Finally, the global shape of the vessel encoded in the parameters of the shape model seems to have no influence on the motion of the Thoracic Aorta after stent-grafting.

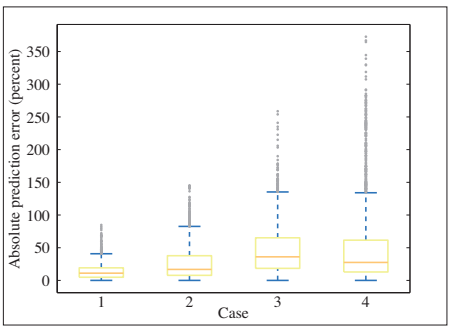

Fig. 1: Prediction error

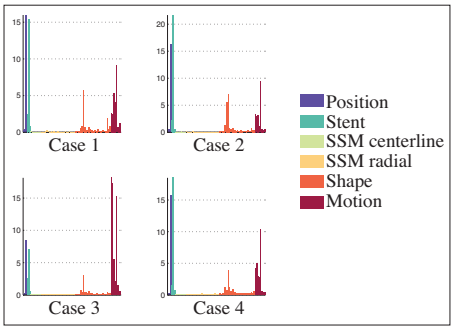

Fig. 2: Feature Importance

5.2 Model accuracy

We evaluate the accuracy of the proposed model of stent-grafting in the Thoracic Aorta in 4 cases with LOOCV. Illustrative plots of the pre-interventional, estimated and post-interventional values of TDT are shown in Figure 3. We computed the prediction error in percent of the absolute values of the change after intervention calculated with the proposed regression model. The mean error over all cases was 32.19%. The mean median error lies at 21.91%, with a mean standard deviation of 29.83%. Figure 1 shows a detailed graph of these results.

5.3 Effects of stent-grafting

By visual inspection of the cases in figure 3, the influence of stent-grafting on the motion of the Thoracic Aorta become apparent. As could be expected due to its closeness to the aortic valve and thus the heart, the strongest vessel movement can be observed in the Ascending Aorta. As previous results indicated [6], introduction of a stent-graft generally reduces the motion in the affected area. In the observed cases, the TDT of the stented area (indicated by the horizontal grey lines in each figure) decreased by 0.96mm on average while the overall decrease was of only 0.5mm. As we previously reported [12], another measurable effect of stent-grafting is the homogenization of the movement in the affected area. In the 4 cases we investigated, the standard deviation in TDT in the stented part of the vessels decreased an average of 1.5mm. However, this effect is not consistent over all cases. Notably, at -0.045mm and $+0.004$mm, the changes in standard deviation in TDT in cases 1 and 2 is negligible. Cases 3 and 4 however show significant changes of $+0.37$mm and -0.5mm respectively. We explain the poorer performance of our prediction model in cases 3 and 4 (at mean error rates of 46% and 49% compared to 14% and 26% in cases 1 and 2) with these large variations in TDT. In these cases, the stent-grafting procedure seems to have led to considerable changes in the homogeneity of the vessel movement that could not be learnt by the proposed method based on the small amount of training data available.

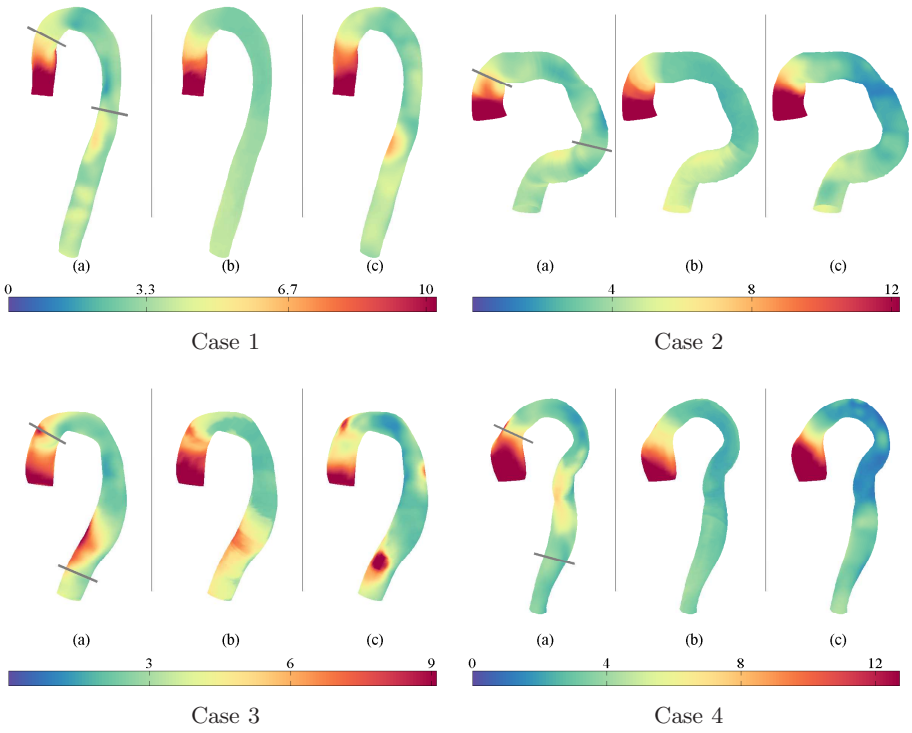

Fig. 3: (a) pre-intervention, (b) predicted post-intervention, and (c) measured post-intervention TDT in mm. Lines indicate the position of the stent-graft.

6 Discussion

In this paper, we present a method that predicts the effects of stent-grafting in the Aortic Arch on the motion of the thoracic aorta. From a set of dynamic surface models, we extract salient features describing local and global vessel shape as well as the motion of the vessel before the intervention. We apply Random Forest Regression to learn a model of the total distance travelled for each point on the surface of the vessel based on these features. We evaluate the proposed method on 4 cases where stent-grafting has been performed after supra-aortic branch transposition.

As previous work [12] indicated, subtle differences in the shape of the stented part of the vessel as well as the location of the prosthesis in the aorta can lead to large variations in the homogeneity of vascular movement after the intervention. Analysis of the error rates on the 4 observed cases confirms these results, as it correlates with the deviation in vascular movement.

Feature importance scores indicate that global shape features seem to have negligible influence on the effects of the stent-grafting procedure when compared

to a priori movement and local geometry of the vessel. In the future, we plan on assessing the locality of vascular movement in more detail. We expect that investigating the interaction between global and local shape features on larger datasets as well as their correlation with vascular movement will lead to a deeper understanding of the relevance of specific geometric properties of the aorta in terms of development and treatment of vascular diseases.

References

1. Gottardi, R., Funovics, M., Eggers, N., Hirner, A., Dorfmeister, M., Holfeld, J., Zimpfer, D., Schoder, M., Donas, K., Weigang, E., Lammer, J., Grimm, M., Czerny, M.: Supra-aortic transposition for combined vascular and endovascular repair of aortic arch pathology. Ann Thorac Surg **86**(5) (Nov 2008) 1524–9
2. van Prehn, J., Bartels, L.W., Mestres, G., Vincken, K.L., Prokop, M., Verhagen, H.J.M., Moll, F.L., van Herwaarden, J.A.: Dynamic aortic changes in patients with thoracic aortic aneurysms evaluated with electrocardiography-triggered computed tomographic angiography before and after thoracic endovascular aneurysm repair: Preliminary results. Annals of Vascular Surgery **23**(3) (Jun 2009) 291–297
3. Muhs, B., Vincken, K., van Prehn, J., Stone, M., Bartels, L., Prokop, M., Moll, F., Verhagen, H.: Dynamic cine-ct angiography for the evaluation of the thoracic aorta; insight in dynamic changes with implications for thoracic endograft treatment. European journal of vascular and endovascular surgery **32**(5) (2006) 532–536
4. Figueroa, C., Taylor, C., Yeh, V., Chiou, A., Gorrepati, M., Zarins, C.: Preliminary 3d computational analysis of the relationship between aortic displacement force and direction of endograft movement. Journal of vascular surgery **51**(6) (2010) 1488–1497
5. Metz, C.T., Klein, S., Schaap, M., van Walsum, T., Niessen, W.J.: Nonrigid registration of dynamic medical imaging data using nd+t b-splines and a groupwise optimization approach. Medical Image Analysis (Nov 2010) 1–12
6. Schwartz, E., Gottardi, R., Holfeld, J., Loewe, C., Czerny, M., Langs, G.: Evaluating deformation patterns of the thoracic aorta in gated cta sequences. Biomedical Imaging: From Nano to Macro, 2010 IEEE International Symposium on (2010) 21–24
7. Heimann, T., Meinzer, H.P.: Statistical shape models for 3d medical image segmentation: A review. Medical Image Analysis **13**(4) (Aug 2009) 543–563
8. Jain, V., Zhang, H.: A spectral approach to shape-based retrieval of articulated 3d models. Computer-Aided Design **39**(5) (2007) 398–407
9. Choi, G., Cheng, C.P., Wilson, N.M., Taylor, C.A.: Methods for quantifying three-dimensional deformation of arteries due to pulsatile and nonpulsatile forces: Implications for the design of stents and stent grafts. Ann Biomed Eng **37**(1) (Jan 2009) 14–33
10. Breiman, L.: Random forests. Machine Learning **45**(1) (2001) 5–32
11. Liaw, A., Wiener, M.: Classification and regression by randomforest. R News 2 **3** (2002) 18–22
12. Schwartz, E., Holfeld, J., Czerny, M., Langs, G.: Visualizing changes in vessel wall dynamics due to stent-grafting in the aortic arch. Biomedical Imaging: From Nano to Macro, 2012 IEEE International Symposium on (2012) to appear